# RMP Colloquia

This section, offered as an experiment beginning in January 1992, contains short articles intended to describe recent research of interest to a broad audience of physicsts. It will concentrate on research at the frontiers of physics, especially on concepts able to link many different subfields of physics. Responsibility for its contents and readability rests with the Advisory Committee on Colloquia, U. Fano, chair, Robert Cahn, S. Freedman, P. Parker, C. J. Pethick, and D. L. Stein. Prospective authors are encouraged to communicate with Professor Fano or one of the members of this committee.

---

# A common mechanism of collective phenomena

U. Fano

*Department of Physics and The James Franck Institute, University of Chicago, Chicago, Illinois 60637*

A common thread is followed through diverse phenomena: Weak interactions lock seemingly independent variables into a collective state of enhanced or depressed energy. A rather novel perspective is thus afforded on superconductivity and on nuclear and particle physics.

## CONTENTS

I. Introduction 313
II. Plasmon Excitation in Condensed Matter 313
A. Empirical macroscopic model 314
B. Long-range interactions 314
C. Dynamics of interaction 315
D. Results and discussion 315
III. Critical Features of the Model Equations (6)–(8) 316
IV. Molecular and Nuclear Analogs 317
V. Superconductivity 318
VI. Relevance to Quark Physics? 319
Acknowledgments 319
References 319

## I. INTRODUCTION

Familiar knowledge of the structure of matter centers on the motion of (quasi)independent particles and on the (quasi)free wavelike propagation of photon and phonon fields. In this context surprise has been elicited by the emergence of phenomena—superconductivity, plasmons, nuclear deformations—that hinge instead on coordination of particles and fields.

Treatments of this coordination, developed in the late 1950s, utilize, in fact, a *single* mathematical mechanism whose manifestations differ in origin and form throughout physics. Common to these phenomena is the role of a dense spectrum of states viewed initially as independent. The seemingly weak interaction among these states often condenses into a single eigenvalue separated from the rest of the spectrum by an energy gap. The present outline of this mechanism and of its manifestations has been stimulated by an indication of its possible role in particle physics, a role that will be touched upon in a final section but that remains nebulous at this time.

The truly macroscopic phenomena mentioned above, plasmons and superconductivity, will be seen to hinge on long-wavelength Fourier components of the Coulomb force, which cement multitudes of electrons and/or nuclei into extended coherent states of aggregation. This cementing action emerges when a suitable index approaches or exceeds unity. Short-range nuclear forces and short-wavelength Coulomb components play the corresponding role for nuclear deformations and for other localized phenomena.

An index that measures the effectiveness of particle-field interactions will be developed analytically for the example of plasmon excitation. Its relevance to other phenomena will then be indicated through qualitative discussion only. Application of this approach to superconductivity will allow us to bypass apparent complexities of the BCS theory, which are rooted in its historical development and persist in current texts. It will also stress the effective strength of interactions over the role of specific mechanisms. Superfluidity will not be dealt with *per se,* but is presumed to differ from superconductivity mainly in that it concerns mass displacements instead of charge displacements.

## II. PLASMON EXCITATION IN CONDENSED MATTER

Collective motions of charged particles are readily analyzed in low-density ionized gases ("plasmas"). Each electron or positive ion moves through the gas with occasional collisions under the influence of the fluctuating field from other particles and of its own inertia. The long range of the Coulomb field provides, however, some coordination. This influence manifests itself through wavelike departures of the electron density from its average value $N$. The frequency

$$\omega_p = (4\pi e^2 N/m)^{1/2} \tag{1}$$

of these oscillations is inversely related to the electron mass $m$, rather than to the larger ion masses. Bohm and

Pines (1953) pointed out that the density of metal electrons should display analogous oscillations, favored by their high mobility. The density $N$ of conduction electrons in metals yields, in Eq. (1), values of $\omega_p$ whose corresponding energy quantum $\hbar\omega_p$—a "plasmon"—is on the order of 10 eV. Plasma excitations should thus be readily apparent in the energy-loss spectra of fast electrons traversing metal foils, a prediction that was promptly verified.

This discovery led to two related questions: (1) How would interband transitions of metal electrons be distinguished from plasmons? (2) Would semiconductors and other nonmetallic materials also display plasmon excitations? Plasmon formation was then shown to emerge from a more comprehensive treatment of the action of Coulomb forces, which coordinates pairs of otherwise independent excitations of outer-shell electrons in condensed matter and yields the Bohm-Pines result as a limiting case (Fano, 1960).

### A. Empirical macroscopic model

The force exerted on a single electron within matter by a weak electric field perturbs the electron but little, eliciting a quasielastic response. This consideration underlies the "electron theory of matter" developed a century ago to describe the linear response ("polarization") of bulk matter to probe fields, e.g., optical radiation (see, for example, Crawford, 1965; Fano and Fano, 1972).

The polarization consists of electron displacements characterized by an empirical spectrum of resonant frequencies $\{\omega_n\}$ whose (generally small) imaginary part $i\gamma_n$ represents inelastic relaxation. To each $\omega_n$ corresponds an "oscillator strength" $f_n$, which represents the fraction of all electrons that participates in the resonance. The dynamics of resonating electrons is represented in terms of their energy, conveniently shorn of irrelevant factors. One such factor is the squared peak displacement of electrons, which depends on the probe-field strength; a second one is the electron mass. The energy thus normalized has the physical dimensions of a *squared frequency*. It can thus be indicated by $\omega_n^2$ for each resonance and by $\omega_p^2$ for a free-electron plasmon. An electric ac field with frequency $\omega$ thus drives each resonant frequency in proportion to the ratio of its response and the mismatch of squared frequencies,

$$\frac{\omega_p^2 f_n}{\omega_n^2-\omega^2} \ . \tag{2}$$

Quantum mechanics reproduces this and other results[1] and complements them by evaluating the spectra of $\{\omega_n\}$ and $\{f_n\}$ for specific atoms, molecules, and crystals. The (complex) dielectric function $\epsilon(\omega)$, i.e., the squared refraction index $n^2$ of the material, is represented in the basic model through the sum over all contributions (2) of its spectrum. Differences among the spectra of $\{\omega_n\}$ and $\{f_n\}$ pertaining to different materials will matter to us only in the context of specific applications. Note that the atomic structures and mechanisms underlying these spectra and the ratio (2) are *not* relevant to the following treatment; therein lies its generality.

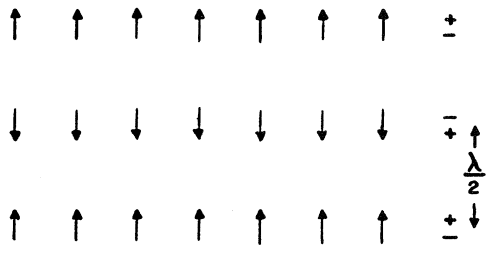


FIG. 1. Diagram of polarization layers in long-wavelength longitudinal excitations traveling along the ordinate axis. Adjacent layers repel each other in this case but attract each other for transverse excitations where all polarization arrows are rotated by 90° clockwise.

### B. Long-range interactions

The Coulomb potential $e^2/|\mathbf{r}_i-\mathbf{r}_j|$ between any two electrons at positions $(\mathbf{r}_i,\mathbf{r}_j)$ correlates their motion in principle. The net effect of this correlation tends to average out for all *distant* pairs in homogeneous isotropic materials and is accordingly disregarded in quantum-mechanical calculations of the parameters $\{\omega_n,f_n\}$. This cancellation is, however, incomplete for the nonuniform polarization induced by probe fields with semimacroscopic wavelength. The net effect of long-range Coulomb correlations remains generally modest in the case of optical radiation, for reasons to be indicated later, but is instead responsible for the excitation of plasmons by Coulomb fields.

The polarization pattern generated by a *longitudinal* ac field $\mathbf{E}_0\exp[i(\mathbf{q}\cdot\mathbf{r}-\omega t)]$, with $\mathbf{E}_0$ parallel to $\mathbf{q}$ and $q=2\pi/\lambda$, is represented schematically in Fig. 1. We consider here the Coulomb interaction of all electron pairs at positions $(\mathbf{r}_i,\mathbf{r}_j)$ in *different* layers of the pattern, expressed as a Fourier integral

$$\frac{e^2}{|\mathbf{r}_i-\mathbf{r}_j|}=\frac{e^2}{2\pi^2}\int d\mathbf{k}\, k^{-2}\exp[i\mathbf{k}\cdot(\mathbf{r}_i-\mathbf{r}_j)] \ .$$

[1]Quantum mechanics treats polarizability or dielectric response by lowest-order perturbation, which introduces a resonance frequency (or energy) difference $\omega_n-\omega$ in Eqs. (2)–(7) instead of $\omega_n^2-\omega^2$. Interference between time-dependent factors $\exp(\pm i\omega t)$ (or between complex conjugate contributions to polarizability in time-independent formulations) yields, however, a second resonance denominator $(\omega_n+\omega)^{-1}$, which generates $(\omega_n^2-\omega^2)^{-1}$ when combined with the initial one. Small values of $\omega_n$, implying close proximity of resonances at $\omega=\pm\omega_n$, thus underlie the boost of spectral concentration of low $\omega$. Reliance on perturbation treatment, rather than on an oscillator model of the zeroth-order states $|n\rangle$, underlies the classical oscillator appearance of Eqs. (2)–(7).

Upon summation over all electron pairs, the contribution from each element of the Fourier integral with $\mathbf{k}\neq\mathbf{q}$ cancels out. A net contribution stems, however, from the single Fourier component with $\mathbf{k}=\mathbf{q}$, i.e., with the *same space distribution as the polarization,* namely,

$$\propto \exp[i\mathbf{q}\cdot(\mathbf{r}_i-\mathbf{r}_j)] \ . \tag{3}$$

This residual interaction, characteristic of a specific polarization pattern, is foreign to the definition and calculations of the parameters $\{\omega_n,f_n\}$ and hence provides an additional contribution to the material's response.

The component (3) of the Coulomb interaction between two electrons splits in turn into separate factors $\{\exp(i\mathbf{q}\cdot\mathbf{r}_i),\exp(-i\mathbf{q}\cdot\mathbf{r}_j)\}$, each of which depends on the position of a single electron. Its action can thus induce *two-electron transitions* with frequencies $(\omega_n,\omega_m)$ and amplitudes proportional to matrix elements of $\exp(\pm i\mathbf{q}\cdot\mathbf{r})$. Each matrix element depends on $\mathbf{q}$ in principle, but this dependence is negligible as long as each electron's position is confined to a range $\ll q^{-1}$ in its calculation. In the limit of $q\to 0$ the residual interaction term (3) thus contributes a factor $f_n^{1/2}f_m^{1/2}$. These circumstances provide the key to a theory of plasmons that encompasses metals and nonmetals (Fano, 1960).

### C. Dynamics of interaction

The normalized excitation energies $\{\omega_n^2\}$ of the macroscopic model may be viewed as elements of a diagonal matrix $\omega_n^2\delta_{nm}$. This energy is now to be complemented, for a polarization proportional to $\exp[i(\mathbf{q}\cdot\mathbf{r}-\omega t)]$, by the contribution of Coulomb components (3). This contribution is represented by the nondiagonal *unit rank* matrix $C\omega_p^2 f_n^{1/2}f_m^{1/2}$, whose structure is analogous to the numerator of Eq. (2). The unit rank of this matrix, i.e., its dependence on $n$ and $m$ through separate factors, stems from our dealing with the effect of a *single,* fully specified, polarization wave. This feature of the interaction is central to the mechanism discussed here. The coefficient $C$ has the alternative values

$$C_l=\tfrac{2}{3} \ , \quad C_t=-\tfrac{1}{3} \ , \tag{4}$$

for the probe-field polarizations parallel or transverse to $\mathbf{q}$, indicated in Fig. 1, which are generated by electron scattering or optical radiation, respectively.

The resulting matrix, $\omega_n^2\delta_{nm}+C\omega_p^2 f_n^{1/2}f_m^{1/2}$, is diagonalized by an orthogonal transformation matrix $a_{\mathcal{N}n}$, each of whose rows represents the $\mathcal{N}$th eigenvector of the equation

$$\omega_n^2 a_n + C\omega_p^2 f_n^{1/2}\sum_m f_m^{1/2}a_m=\omega^2 a_n \ . \tag{5}$$

This transformation replaces the macroscopic model's parameters $\{\omega_n,f_n\}$ as required by the addition of long-range interactions: The eigenvalues $\omega\equiv\Omega_{\mathcal{N}}$ of Eq. (5) replace the $\omega_n$, and the oscillator strengths $F_{\mathcal{N}}=|\sum_n a_{\mathcal{N}n}f_n^{1/2}|^2$ replace the $f_n$.

The structure of Eq. (5) enables us to transform it into

$$a_n=-\frac{C\omega_p^2 f_n^{1/2}}{\omega_n^2-\omega^2}\sum_m f_m^{1/2}a_m \ . \tag{6}$$

Multiplication of Eq. (6) by $\sum_n f_n^{1/2}$ provides the eigenvalue equation to be solved,

$$-C\omega_p^2\sum_n\frac{f_n}{\omega_n^2-\omega^2}=-C\alpha(\omega)=1 \ . \tag{7}$$

The coefficient $\alpha(\omega)$—equivalent to $4\pi\chi$ of Crawford (1965)—represents the polarizability of a unit volume of the material in the absence of long-range Coulomb interactions, in which case $\epsilon(\omega)=1+\alpha(\omega)$. The presence of these interactions replaces this relation by the Clausius-Mossotti formula,

$$\epsilon(\omega)=\frac{1+2\alpha(\omega)/3}{1-\alpha(\omega)/3} \ . \tag{8}$$

### D. Results and discussion

The occurrence of plasmon-type collective oscillations in the energy-loss spectrum of charged particles—and of analogous effects to be discussed later—will now be shown to rest on comprehensive features of the polarizability function, Eq. (7), illustrated in Fig. 2. These features involve the density $N$ of outer-shell electrons (a factor of the coefficient $\omega_p^2$) and their spectral parameters $(\omega_n,f_n)$. We shall first indicate significant features of $\alpha(\omega)$ in spectral ranges where the oscillator-strength density is either very low or very high, and then point out their interplay when high and low densities prevail in adjoining spectral ranges:

(a) A frequency range in which the density of oscillator strength is low is characterized by

$$\frac{\omega_p^2 f_n}{|\omega_n^2-\omega_{n\pm1}^2|}\ll 1 \ . \tag{9}$$

Equation (7) has in this case a perturbative solution,

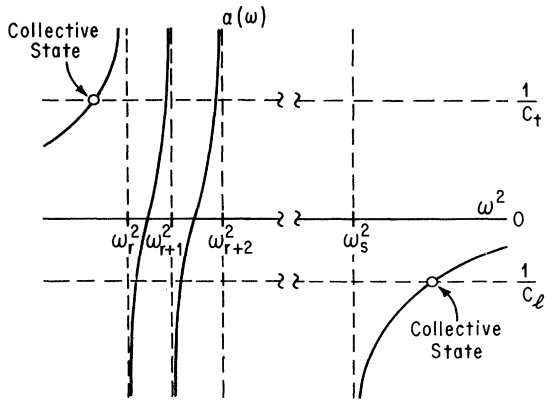


FIG. 2. Qualitative representation of the polarizability function $\alpha(\omega)$ and of graphic solutions of Eq. (7) as described in the text.

namely, $\omega^2 \sim \Omega_n^2 = \omega_n^2 + C\omega_p^2 f_n$, since terms of $\alpha(\omega)$ with $m \neq n$ contribute negligibly at $\omega^2 \sim \omega_n^2$. The frequency shift $\Omega_n^2 - \omega_n^2$, however small, combines the density $N$, the charge and the mass of electrons, through $\omega_p^2$, and the oscillator strength $f_n$ which couples each resonance to a probe field.

(b) In the opposite case

$$\frac{\omega_p^2 f_n}{|\omega_n^2 - \omega_{n\pm1}^2|} \gg 1 , \tag{10}$$

a root of Eq. (7) also occurs near the middle of each interval between $\omega_n$ and $\omega_{n\pm1}$, where $\alpha(\omega)$ traverses its whole range $-\infty < \alpha(\omega) < \infty$. However, the $\sum_m f_m^{1/2} a_m$ in Eq. (6) includes in this case contributions of comparable magnitude and opposite sign from terms with $m < n$ and $m > n$, respectively, whereby the magnitude of the relevant eigenvector, $\sum f_n^{1/2} a_n$, is sharply reduced by *destructive interference.*

(c) The feature of Eq. (7) directly responsible for a major collective phenomenon results when Eq. (10) holds throughout a limited spectral range $\omega_r < \omega < \omega_s$, whereas Eq. (9) holds in adjoining ranges. Whichever fraction of the overall coupling among initially independent oscillators, as represented by $\omega_p^2 \sum_{n=r}^{s} f_n$, lies in this range, destructive interference prevents its local manifestation. In contrast, its contribution

$$\alpha^{(rs)}(\omega) = \omega_p^2 \sum_{n=r}^{s} \frac{f_n}{\omega_n^2 - \omega^2} \tag{11}$$

to the total polarizability $\alpha(\omega)$ proves decisive where the terms of the sum in Eq. (11) *interfere constructively,* that is for $\omega > \omega_s$ and for $\omega < \omega_r$.

The magnitude of $|\alpha^{(rs)}(\omega)|$ remains $\geq 1$ for a considerable spectral range above $\omega_s$ and below $\omega_r$ (provided $\omega_r \neq 0$). Throughout this extended range, its contribution to $\alpha(\omega)$ remains dominant and may be fitted approximately to that of a single "effective oscillator" with frequency $\omega_{\text{eff}}$ and strength $f_{\text{eff}} \sim \sum_{n=r}^{s} f_n$,

$$\alpha(\omega) \sim \alpha^{(rs)}(\omega) \sim \frac{\omega_p^2 f_{\text{eff}}}{\omega_{\text{eff}}^2 - \omega^2} . \tag{12}$$

On this basis, Eq. (7) predicts the occurrence of a high-intensity "collective" normal mode with the eigenfrequency

$$\Omega_{\text{eff}}^2 \sim \omega_{\text{eff}}^2 + C\omega_p^2 f_{\text{eff}} , \tag{13}$$

which "peels off" the range $\omega_r < \omega < \omega_s$ where Eq. (10) holds. The plasmon frequency is predicted by this formula with the "longitudinal" value $C = \frac{2}{3}$; more precisely, this frequency is the value of $\omega$ at which the Clausius-Mossotti $\epsilon(\omega)$, Eq. (8), vanishes. A corresponding transverse normal mode occurs at the $\omega < \omega_r$ value where $\epsilon(\omega)$ diverges.

The plasmon frequency often exceeds $\omega_s$ by far because the values of $\alpha(\omega)$ and $\epsilon(\omega)$, initially large and negative at $\omega \sim \omega_s$, decrease in magnitude slowly as $\omega$ increases. By contrast the eigenvalues $\Omega_N$ of Eq. (7) for transverse modes ($C_t = -\frac{1}{3}$) appear to depart from the spectrum of $\omega_n$ much less than do the longitudinal eigenvalues. Several circumstances, including the sign and magnitude of $C_t / C_l$, may contribute to this phenomenon.

In metals, the valence electrons contribute a spectrum $\{\omega_n\}$ lying at very low frequencies, with $\omega_r = 0$, thus yielding a longitudinal mode with the plasma frequency (1) and no opportunity for a transverse mode. In semiconductors and insulators both a longitudinal and a transverse plasma mode may occur, provided Eq. (10) holds over a sufficient range. An important aspect of this condition is that *details of the spectrum of* $(\omega_n, f_n)$ *are irrelevant.* The condition itself may be cast in terms of the mean value,

$$\frac{1}{\omega_s - \omega_r} \int_{\omega_r}^{\omega_s} \frac{d(\omega_p^2 f)}{d(\omega^2)} d\omega > 1 , \tag{14}$$

of the oscillator-strength density in space and squared frequency. The spectral density of the oscillator strength of outer-shell electrons meets this condition for some but not for all nonmetallic condensed materials. Since the spectral-density operator $d/d(\omega^2)$ in Eq. (14) is equivalent to $(2\omega)^{-1} d/d\omega$, it boosts the density at low frequencies and depresses it at high frequencies. Accordingly, condition (14) holds mainly for chemically unsaturated materials that absorb light heavily at rather low frequencies; it does not hold at all for inner-shell electrons.

## III. CRITICAL FEATURES OF THE MODEL EQUATIONS (6)–(8)

The mathematical model used above to describe the formation of plasmon resonances may also deal with any base set of states $|n\rangle$ that are stationary with energies $\hbar\omega_n$ in an initial approximation. The nature and localization in space of these states is *not* relevant. Equation (5) introduces a Coulombian coupling between these states represented by the *factored matrix* $C\omega_p^2 f_n^{1/2} f_m^{1/2}$.

Equation (5) itself may be viewed as the Schrödinger equation for a set of coupled states of a system held near equilibrium by linear restoring forces (Crawford, 1965, Chap. 3).[1] This treatment is appropriate to systems whose energy variations are small as compared to their total energy, even though these variations entail conspicuous effects. [See, for example, Sec. II and Eqs. (12)–(19) of Fano (1956).] Alternatively, Eq. (5) may represent the long-range equation for normal modes of coupled oscillators. Equation (6) represents the solution of Eq. (5) in terms of the single "collective variable" $F_N = \sum_m f_m^{1/2} a_m$; Eq. (7) formulates the relevant eigenvalue problem.

Under the condition (14) the value of $|\sum_m f_m^{1/2} a_m|$ peaks for a single isolated eigenvalue of Eq. (7) and is quenched for the other eigenstates, which thus become

hardly observable. The alternative values (4) of the factor $C$ in Eq. (5) boost or lower the total energy, respectively; they correspond to interactions between dipoles lying nose-to-tail or side-by-side, respectively (Fig. 1).

The most critical element for the formation of plasmons—or of analogous states—lies in Eq. (14)'s requirement that there be a high spectral concentration of the coupling among base states, that is, that there be a *high density of quasidegenerate states* interacting through the Coulomb field. This requirement hinges in turn on the value of a dimensionless index, namely, the integrand of (14) or its analog in other phenomena. Notably such indices may take alternative forms depending on the choice of alternative sets of independent variables, as illustrated by replacing the set $\{\omega_p, f, \omega\}$ that occurs in Eq. (14).[2] Such alternatives provide different perspectives on the same phenomenon.

Regardless of the perspective, a value of the critical index comparable to—or larger than—unity implies a strength of interactions that causes the initial description of a system to be replaced by a new one. That perturbation of a (quasi)degenerate base yields eigenstates of different character is, of course, familiar. That a *single eigenstate* is readily observed and most strongly shifted in energy is instead a feature of *factorable perturbations* [i.e., of interactions that link the amplitudes $a_m$ and $a_n$ in the second term of Eq. (5) through a product coefficient $f_n^{1/2} f_m^{1/2}$].

## IV. MOLECULAR AND NUCLEAR ANALOGS

Whereas plasmons in condensed matter result from the interaction of a macroscopic number of particles, plasmonlike spectral features also occur in modest-size aggregates of particles interacting through Coulomb or nuclear forces. Dimers of flat dye molecules, bound to one another face-to-face by a weak van der Waals force, afford a notable example. Incident light drives electron oscillations within the parallel planes of the two molecules, generating dipole moments that repel each other by oscillating in phase but that would attract each other if out of step. Each excited level of a single molecule thus splits into a doublet of the dimer's spectrum, with excitation amplitudes that add up for the higher energy level and cancel for that of lower energy. The enhanced frequency and enhanced intensity of the dimer's main absorption line parallel the plasmon features[3]; they reflect a correlation between electron distributions in the two molecules of opposite sign to the correlation that prevails in their ground state and generates the van der Waals (Kasha *et al.*, 1961). Dye polymers of increasing size display higher and higher concentrations of photoabsorption in the highest frequency line of a band regardless of the integrand's value in Eq. (14). This phenomenon becomes even more conspicuous in molecular crystals, where it has been studied early and in detail (Davydov, 1962).

Joint enhancement—and alternative depression—of frequency and intensity in photoabsorption occur also in the prototypical joint excitation of the helium electrons. Alternative configurations, $(nl,n'l')$ and $(nl',n'l)$, are quasidegenerate in energy in this case. Electron repulsion replaces them by superpositions $(nl,n'l')\pm(nl',n'l)$ (Madden and Codling, 1963, and Cooper *et al.*, 1963).

In atomic nuclei, photoabsorption by the familiar dipole process failed to be observed until ~20 MeV photons became available. It was then pointed out that this high energy is indeed required to separate the center of mass of the protons from that of the neutrons (Goldhaber and Teller, 1948). Independent particle models suggested, on the other hand, that lower-energy photons would suffice to induce a dipole transition of a single proton. These two approaches were later reconciled by observing, in effect, that excited levels of a single proton correspond to the $|n\rangle$ states considered here; their coupling by a dipole component of nuclear forces $Vf_n^{1/2}f_m^{1/2}$ generates the previously predicted higher-energy collective oscillation of protons and neutrons analogous to the plasmon (Brown and Bolsterli, 1959).[4] The selection of this single multipole component, appropriate to the interaction of a long-wavelength radiation with a small nucleus, corresponds to the selection of the polarization component $(\mathbf{q},\omega)$ appropriate to plasmon excitation by scattering of a fast electron in a homogeneous material.

This view extends to most excitations of nuclei, classified by their multipolarity and governed by *factorable* multipole operators such as $P_L(\hat{r}_i\cdot\hat{r}_j)$

---

[2]An alternative form of the integrand in Eq. (14) replaces the oscillator strength symbol $f_n$ utilized in earlier equations by its quantum-mechanical expression in terms of the matrix element for a dipole transition with frequency $\omega_n$, directed along the vector $\mathbf{q}$ of Eq. (3)

$$f_n = 2m\omega_n |(n|\hat{\mathbf{q}}\cdot\mathbf{r}|0)|^2/\hbar \ .$$

When we enter this expression, for example, in Eq. (10), its factor $m$ cancels the electron mass in the denominator of $\omega_p^2$, and the ratio $2\omega_n/|\omega_n^2-\omega_{n+1}^2|$ reduces to $1/|\omega_n-\omega_{n\pm1}|\equiv 1/\Delta\omega_n$, if $\Delta\omega_n \ll \omega_n$. The ratio on the left of Eq. (10) becomes thus

$$4\pi N|(n|e\hat{\mathbf{q}}\cdot\mathbf{r}|0)|^2/\hbar\Delta\omega_n \ ,$$

an expression equivalent to the integrand in Eq. (14). Its numerator represents the electrostatic potential energy of a pair of dipoles at a distance $\sim N^{-1/3}$; its denominator represents the interval of adjacent spectral levels. The ratio itself thus amounts to the interaction energy of a pair of dipoles whose strength is normalized per unit energy.

[3]The factor of $C$ of Eqs. (4)–(7) pertaining to long-range dipole interactions with Fourier components $\exp(i\mathbf{q}\cdot\mathbf{r})$, does not occur in the case of small aggregates where $\mathbf{q}\cdot\mathbf{r}\ll 1$.

[4]Figure 2 of Brown and Bolsterli (1959) may be viewed as a schematic plot, analogous to Fig. 2, of the $\alpha(\omega)$ in Eq. (7), as may the plot on p. 31 of Schrieffer (1964). This coincidence gave rise to the present essay.

$\propto \sum_M Y_{LM}(\hat{r}_i) Y^*_{LM}(\hat{r}_j)$. Much of the spectral density for each multipolarity is indeed concentrated in a "giant $2^L$-pole" resonance analogous to that first envisaged for the oscillation of neutron and proton centers.

Multipole moments of nuclei are studied not only in connection with transitions to excited states but also as observable parameters of ground states. Attention was directed by Bohr and Mottelson long ago to nonzero nuclear quadrupole moments, i.e., to anisotropy of the inertia tensor in a freely rotating reference frame. Here again one may expand the nuclear potential into factorable multipole components; a major contribution accrues from the Coulomb repulsion between protons, which favors a prolate nuclear shape. The action of each multipole component on an initial base set $|n\rangle$ of Hartree-Fock states can thus often generate a collective eigenstate $\sum_n |n\rangle a_n$ with energy substantially lower than the lowest $\omega_n$, depending on the magnitude of the integral in Eq. (14). A suitable formulation of the relevant parameters utilizing hyperspherical coordinates has been developed by Filippov (1973), but apparently with scarce implementation.

## V. SUPERCONDUCTIVITY

London and London (1935) have attributed phenomenologically the onset of superconductivity in condensed materials to the formation of macromolecules, throughout which valence electrons can circulate freely, that is, without dissipating any kinetic energy to the motion of atomic cores. Recall, in this connection, some relevant characteristics of familiar molecules, such as benzene: (1) The spins of valence electrons are paired into singlets, thus enhancing the flexibility for each pair to optimize the bonds among atomic cores. (2) The stronger are these bonds, the higher their vibrational levels within the molecule and the less likely their excitation by electron motions. (3) The onset of a magnetic field generates a circulating current, directed so as to reduce the magnetic flux through the molecule. The BCS theory of superconductivity has shown how long-range correlations of valence electrons and atomic cores, mediated within metals by long-range elastic ("phonon") interactions, extend these properties to macroscopic volumes.

The initial step of the BCS analysis usually deals with circumstances that favor the pairing into spin singlets of electrons in Bloch states with wave vectors $\pm\mathbf{k}$ of equal magnitude and opposite direction ("Cooper pairs"). Departing somewhat from this precedent at the outset, we treat here the pairing of electrons with momenta $\pm\mathbf{k}$ and with independent spins as energetically neutral, that is, as a mere rotation of Hilbert-space coordinates. This rotation replaces each pair of two-electron wave functions

$$\langle \mathbf{r}_1 | \pm\mathbf{k}, m_s = \pm\tfrac{1}{2} \rangle \times \langle \mathbf{r}_2 | \mp\mathbf{k}, m_s = \mp\tfrac{1}{2} \rangle \ , \tag{15a}$$

conjugate under time reversal ($\pm \rightarrow \mp$), by the pair of singlet and triplet functions

$$\begin{aligned} &\langle \mathbf{r}_1 - \mathbf{r}_2 || \mathbf{k} |, S = 0 \rangle \propto \cos[\mathbf{k}\cdot(\mathbf{r}_1 - \mathbf{r}_2)] \ , \\ &\langle \mathbf{r}_1 - \mathbf{r}_2 || \mathbf{k} |, S = 1 \rangle \propto \sin[\mathbf{k}\cdot(\mathbf{r}_1 - \mathbf{r}_2)] \ . \end{aligned} \tag{15b}$$

The singlet wave function has an antinode at $\mathbf{r}_1 = \mathbf{r}_2$, which allows both electrons to lie at a position of lowest potential as they do in a molecular bond. It also represents a state of zero velocity of the pairs' center of mass, whose position thus affords easier correlation with slowly oscillating atomic cores. (The triplet wave function no longer concerns us.)

Following this preliminary modification of a key feature of BCS superconductivity, the theory may follow a course parallel to that of plasmon theory. Each state $|n\rangle$ of the initial approximation is now the product of a singlet two-electron state (15b) and a phonon state with wave vector $\mathbf{K}$, i.e., $|n\rangle \equiv ||\mathbf{k}| S \mathbf{K}\rangle$. Pairs of states $(|n\rangle, |n'\rangle)$ with $S = S'$ are then coupled by plane-wave components [Eq. (3)] of the Coulomb field, where $(\mathbf{r}_i, \mathbf{r}_j)$ indicate here the positions of an electron *pair* and of an atomic core instead of the positions of two separate electrons. Diagonalizaton of the resulting Hamiltonian then proceeds through an equation analogous to Eq. (5). An obvious difference lies, of course, in the predominance here of the attraction between electrons and atomic cores over the electron-electron repulsions. This predominance, represented by a *negative value* of $C_l$ in Eqs. (5)–(7), pushes the BCS correlated level of the *singlet* submatrix ($S = 0$) below the spectrum of uncoupled levels $\omega_n$. Common to the theory of metal plasmons is the role of near-zero frequencies that boost the spectral concentration $d(\omega_p^2 f)/d(\omega^2)$ of quasidegenerate uncoupled levels. Indeed the low values of $T_c$ in BCS superconductivity imply that condition (14) holds only for an extremely narrow range of frequencies, from $\omega_r \sim 0$ to $\omega_s \sim k_B T_c/\hbar$.

A departure from the factoring of interaction in Eq. (3) is suggested for BCS theory by the clustering of electron states near the Fermi surface. The Fourier analysis of the Coulomb interaction is replaced conveniently by its multipole analysis in wave-vector space, as presented on p. 29 of Schrieffer (1964). This variant appears, however, inessential.

The original BCS formulation has been primarily concerned with the structure and transformations of the spectrum of zeroth-order states, possibly for historical reasons. It has also relied heavily on field-theoretical analysis to demonstrate the energetic instability of the zeroth-order spectrum $\{\omega_n\}$ [see chapters 5–7 of Schrieffer (1964)]. The plasmon formulation presented here stresses instead effective parameters of the interaction, such as appear in Eqs. (12)–(14), whose values depend mainly on the spectral concentration of the interaction but only weakly on its spectral details. No evaluation of the analogs of Eqs. (12)–(14) for the theory of superconductivity is attempted here.

The present variant of BCS theory views the "energy gap" as a spectral feature of the electron + phonon sys-

tem, rather than as a result of the system's instability at low temperatures. We have dealt here only with the system's spectrum, anticipating that the electrons will condense at low temperatures into the isolated and depressed ground state, in thermal equilibrium with the spectral levels above the gap. (These contrasting aspects of the present variant and of the original BCS theory have come into focus through a conversation with G. Strinati.)

The BCS theory succeeded rather quickly in relating quantitatively the energy gap and other main properties of the superconducting state to the electron and phonon spectra of simple metals. The corresponding endeavor for high-$T_c$ superconductors has not yet been successful. Efforts to identify and evaluate the analogs of Eqs. (12)–(14) for the far richer and more complex spectra of high-$T_c$ materials might prove fruitful, by stressing the spectral density and the *average* coupling among the $|n\rangle$ states rather than the role of specific mechanisms. The wealth and diversity of bonding and of vibronic structures within unit cells of the high-$T_c$ crystals will, of course, hinder this evaluation. They will, on the other hand, greatly enlarge the range of factors capable of boosting $T_c$ by an order of magnitude.

## VI. RELEVANCE TO QUARK PHYSICS?

The current "Standard Model" of particle physics deals with three pairs of quarks of different flavors, namely, $(d,u)$, $(s,c)$, and $(b,t)$, whose effective masses we discuss here. Values of these masses are estimated indirectly for the three lightest ones, "down," "up," and "strange;" they lie below 1 GeV/$c^2$. For "charm" and "bottom," the mass values stem instead directly from the observed energy of the resonant states $J/\psi$ and $\Upsilon$ that decay into quark-antiquark pairs, $(c,\bar{c})$ and $(b,\bar{b})$. These values are

$$M_c \sim 1.5 \text{ GeV}/c^2 , \quad M_b \sim 5 \text{ GeV}/c^2 . \tag{16}$$

The last, "top" quark has never been detected experimentally, presumably because its much larger mass, on the order of $\sim 100$ GeV/$c^2$, has prevented its detection by present-day facilities. The occurrence of a mass—equivalent to an energy eigenvalue—exceeding the other masses by 1–2 orders of magnitude suggests as a working hypothesis that it might originate from much the same mechanism as the plasmon energy. The high spectral density of hadronic states below 5 GeV, classified by several multivalued quantum numbers, would provide a necessary ingredient. A recent scoring of this density yields 267 meson states and 740 baryon states in the energy range between 1 and 2 GeV ( Freund and Rosner, 1991). In this view the quark masses correspond to the eigenvalues $\Omega_N$ of Eq. (8), rather than to the $\omega_n$. Note that the Standard Model parametrizes the quark masses in terms of observables currently inaccessible to experiment, but does not relate them directly to the rich phenomena observed in the energy range of order 1 GeV. The interactions among quarks are short range, of course, as for nuclei, but even stronger and less well known at this time.

This remark and indeed this whole article originate from an earlier suggestion by Nambu (1989) concerning the possible role of a $(t,\bar{t})$ resonance—the flavor partner of the $\Upsilon$—as a Higgs boson. This boson field in turn would follow the model of BCS superconductivity. The large energy gap separating this resonance from the other hadron levels would stem from manifold interactions interfering constructively along a single degree of freedom. Appropriate analysis of the manifold current evidence on hadron interactions might serve to assess this approach.

## ACKNOWLEDGMENTS

This paper owes much to stimulation and advice by numerous colleagues. It was prepared with partial support by the NSF Grant PHY 90-19966.

## REFERENCES

Bohm, D., and D. Pines, 1953, Phys. Rev. **92**, 609.
Brown, G. E., and M. Bolsterli, 1959, Phys. Rev. Lett. **3**, 472.
Cooper, J. W., U. Fano, and F. Prats, 1963, Phys. Rev. Lett. **10**, 518.
Crawford, F. S., 1965, *Waves* (McGraw-Hill, New York), p. 563 ff.
Davydov, A. S., 1962, *Theory of Molecular Excitons* (McGraw-Hill, New York).
Fano, U., 1956, Phys. Rev. **103**, 1202.
Fano, U., 1960, Phys. Rev. **118**, 451.
Fano, U., and L. Fano, 1972, *Physics of Atoms and Molecules* (University of Chicago, Chicago).
Filippov, G. F., 1973, Fiz. Elem. Chastits. At. Yadra **4**, 992 [Sov. J. Part. Nucl. **4**, 405 (1974)].
Freund, P. G. O., and J. L. Rosner, 1991, unpublished.
Goldhaber, M., and E. Teller, 1948, Phys. Rev. **74**, 1046.
Kasha, M., M. Ashraf El Bayoumi, and W. Rhodes, 1961, J. Chim. Phys. **58**, 196.
London, F., and H. London, 1935, Proc. R. Soc. London, Ser. A **149**, 71.
Madden, R., and K. Codling, 1963, Phys. Rev. Lett. **10**, 516.
Nambu, Y., 1989, in *Forty Years of Rochester Conferences,* edited by Ashok Das (World Scientific, Singapore, 1991), p. 1.
Schrieffer, J. R., 1964, *Theory of Superconductivity* (Benjamin, Reading, MA).